# Drawability of Ultrahigh Molecular Weight Polyethylene Single-Crystal Mats

**Tetsuya Ogita,† Yoshihisa Kawahara,† Ryouhei Nakamura,† Takeshi Ochi,† Masatomo Minagawa,† and Masaru Matsuo*,‡**

*Department of Materials Science and Engineering, Faculty of Engineering, Yamagata University, Yonezawa 992, Japan, and Department of Clothing Science, Faculty of Home Economics, Nara Women's University, Nara 630, Japan*

*Received November 23, 1992; Revised Manuscript Received April 26, 1993*

ABSTRACT: Single-crystal mats of ultrahigh molecular weight polyethylene were successfully prepared from *p*-xylene solution for studies of the influence of chain entanglement on the drawability of these mats. In the microscopic levels observed for small-angle X-ray scattering and scanning electron microscopy, films prepared from the mats had a morphology similar to that of dried gel films that were prepared by the usual procedure. The maximum attainable draw ratio was well in excess of 200 if the specimen was annealed at 130–140 °C and stretched at the same temperature. But it was only about 10 when the specimen annealed at 140 °C, slightly above the melting point, was stretched at 20 °C. This draw ratio at 20 °C was one-third of the annealed gel films prepared from solutions with their optimum concentration. On the other hand, single-crystal mats prepared by a new procedure to minimize the number of entanglement meshes showed a wide variation in the drawability, ranging from 0 to 150 depending on the temperature at which the specimens were stretched. However, the compressed mats could not be elongated at room temperature without the annealing at 140 °C. These results support the hypothesis that the suitable number of chain entanglements plays an important role in transmitting the tensile force effectively during the drawing.

## Introduction

Since 1974, polymeric fibers and films with high strength and high modulus have been prepared by several methods including gel state spinning,[1] ultradrawing of dried gel films,[2,3] and ultradrawing of single-crystal mats.[4,5] Interesting results have been obtained for polyethylene and polypropylene. In particular, the Young's modulus of ultradrawn polyethylene is more than 200 GPa which is close to the Young's modulus of supersteel.[3]

Smith et al.[6] developed the gel deformation method and demonstrated that the drawability of ultrahigh molecular weight polyethylene (UHMWPE) could be dramatically enhanced if the specimens were spun or cast from macroscopic gels prepared from semidilute solutions. For a sufficiently high molecular weight, the maximum achievable draw ratio depended principally on the concentration of the solution from which the gel was made.[7] This phenomenon was attributed to the smaller number of entanglements per molecule in solution-cast/spun specimens than in the melt-spun specimens.

The drawing of single-crystal mats that were prepared from low molecular weight polyethylene (LMWPE) has yielded some interesting results. Statton studied the drawing behavior of single-crystal mats that were annealed at 110 °C to examine the heating effects on the coherence of lamellar crystals.[8] Ishikawa et al. succeeded in the drawing of single-crystal mats with draw ratios over 30 at temperatures higher than 90 °C.[9-11] Unfortunately, the mechanical properties of these drawn mats were poor. Following the successful fabrication of high-modulus fibers by gel spinning using UHMWPE,[1-3] Miyasaka et al.[4] and Kanamoto et al.[5] tried to elongate ultradrawn single-crystal mats of UHMWPE that had been pressed at high temperatures. In these studies, they were able to draw the compressed mats up to a draw ratio of 300. The Young's modulus was greater than 200 GPa which was comparable to the value obtained from the drawn gel films.

In a previous paper,[12] we reported that sheets of the LMWPE gels tended to break up into flakes rather than form films while being dried. Since these gels are highly crystallizable (crystallinity >80%), the flaking phenomenon may be attributed to the small number of entanglements brought about by the relatively short segments in each molecule that are available for the formation of an amorphous phase.

It may be noted that, if the single-crystal mats of UHMWPE prepared by Miyasaka et al.[4] and Kanamoto et al.[5] had the same rhombic shape as the single crystal of LMWPE, there should be very few, if any, entanglements in the crystal mats because the surface of the crystal would contain only regular folded chain loops. Accordingly, Kanamoto et al.[5] attributed the high drawability of the resultant films to chain cohesion instead of chain entanglements in the film.

It is, therefore, of interest to critically examine whether chain entanglements are essential for the high drawability as suggested by Smith et al.,[6] in spite of the difficulty in estimating the entanglement density directly. Accordingly, we tried to prepare single-crystal mats of UHMWPE having varying degrees of entanglements by using several methods in this paper. The preparation of these mats is due to an indirect means of studying their morphology and deformation mechanism in relation to the number of entanglements within the specimens by means of small-angle X-ray scattering (SAXS), wide-angle X-ray diffraction (WAXD), and scanning electron microscopy (SEM).

## Experimental Section

**Sample Preparation.** Single-crystal mats were prepared from linear polyethylene with molecular weights $3 \times 10^6$ (Hizex Million 240M), $1 \times 10^6$ (Hizex Million 145M), and $3 \times 10^5$ (Sholex Super 5551H). The polymer was dissolved in *p*-xylene with a concentration of either 0.1 or 0.01 g/100 mL. The solutions were stabilized with 0.1% w/w of an antioxidant di-*tert*-butyl-*p*-cresol. *p*-Xylene solutions of these polymers were prepared by heating the polymer/solvent mixture at 135 °C under an entrainment of nitrogen gas. The homogenized solution together with the holding flask was quenched in running water and heated again at 135 °C for 15 min following the procedure of Kanamoto et al.[5] The

* To whom all correspondence should be addressed.
† Yamagata University.
‡ Nara Women's University.

0024-9297/93/2226-4646$04.00/0 

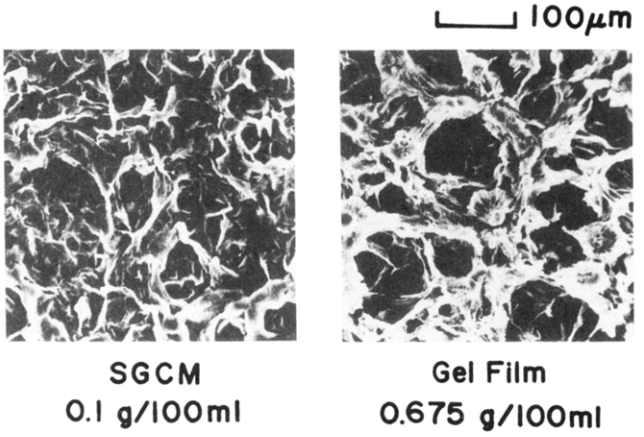


**Figure 1.** SEM photographs of type I single-crystal mats and gel film prepared from solutions with concentrations of 0.1 and 0.675 g/100 mL, respectively.

mixture was cooled slowly to 85 °C and kept there for 24 h to achieve isothermal crystallization. Afterward, the solution was slowly cooled to room temperature.

The crystal-containing solution was then dried in two different ways as described below.

**Method I.** The solution was poured onto a glass filter, and the residual solvent was allowed to evaporate under ambient conditions. This procedure was essentially the same as the one reported by Kanamoto et al.[5]

The dried mats had a texture which resembled that of the dried gel films rather than the single-crystal mats of LMWPE. This can be seen from the SEM photographs (Figure 1) of the single-crystal mats (left-hand side) that were prepared by the present method from a 0.1 g/100 mL solution and of a dried gel film (right-hand side) which was prepared by quenching the solution at 0 °C and drying under ambient conditions.[13] As reported earlier,[14] 0.675 g/100 mL was the optimum concentration that gave the maximum draw ratio of the dried gel film. The textures of both specimens were apparently composed of fibrillar interconnected lamellar crystals when viewed edgewise. The single-crystal mats could be elongated to more than 200 times the original length at 130 °C.

It was obvious from the similarity in their morphologies (and their levels of chain entanglements) that we could not meaningfully study the effect of entanglement on the drawability from these two types of specimens. Accordingly, we attempted a slight variation in the specimen preparation procedure to see if this would suppress the number of entanglement meshes and hence the drawability of the specimens. To this end, we individually picked out the wet mat pieces from the glass filter after the homogeneous solution was poured onto the filter; the pieces were then placed apart from each other on a glass plate. The dried pieces were gathered and pressed under pressures of 1–20 MPa at 20 °C. The resultant films were translucent, but again, as with the specimens prepared by the previous procedure, they could be elongated beyond 200 times. Therefore, only a few specimens prepared by this last procedure were used in the experiment. Henceforth, specimens prepared by the procedures described above will be referred to as type I specimens.

**Method II.** This method was adopted as a new attempt to minimize the number of entanglement meshes in the specimen. Before the homogenized solution was poured onto the glass filter, an excess amount of ethanol was introduced into the flask at 20 °C and the mixture was stirred vigorously for 24 h at room temperature. Following the decantation, the solvent mixture was drained and fresh ethanol was introduced again. The treatment was repeated five times to completely purge *p*-xylene from single-crystal mats. The mats were recovered by pouring the solution onto a glass filter. To avoid overlapping of the mats, they were scattered on a glass plate and dried under ambient conditions. Subsequently, the specimen was vacuum-dried for 1 day at room temperature to remove the residual trace of solvent. The single-crystal mats, which were in the powder form, were gathered and pressed into films under the desired compressive stresses. The resultant films were brittle and occasionally broke during handling. All solutions used in method II had a fixed concentration of 0.01 g/100 mL. Specimens prepared by this method are designated as type II specimens.

**Sample Characterization.** Densities of the films were measured by a pycnometer using a mixture of chlorobenzene and toluene. Since the density was very sensitive to the presence of the residual antioxidant, great care was taken to remove the latter. To achieve this, the specimens were immersed in ethanol for more than 10 days and subsequently vacuum-dried for 1 day prior to measurement. The crystallinity was calculated by using 1.000 and 0.852 $g \cdot cm^{-1}$ as densities of the crystal and amorphous phases, respectively.[15]

The thermal property was determined from the endotherms of the DSC curves. Specimens weighing about 3 mg were placed in a standard aluminum dish and heated at a constant rate of 10 $°C \cdot min^{-1}$. SEM photographs and SAXS and WAXD patterns were obtained using the methods described elsewhere.[16] Transmission electron micrographs (TEM) were taken for single-crystal mats of LMWPE ($\bar{M}v = 3 \times 10^5$) and UHMWPE ($\bar{M}v = 1 \times 10^6$) using a Hitachi H-800.

The long period was estimated by densitometer tracings as an optical density distribution from the X-ray films with the small collimator.

## Results and Discussion

Figure 2 shows the WAXD and SAXS patterns (end view) of types I and II single-crystal mats. The incident beam was directed parallel to the mat surface as shown in this figure. To obtain the patterns, the mats were pressed at the indicated pressures at 20 °C. Patterns a–c show that the specimens were composed of single-crystal mats that were oriented with their flat faces parallel to the film surface; the *c*-axes were oriented perpendicularly to the flat faces. These profiles resemble those observed in dried gel films. By contrast, the WAXD pattern d for the type II mats, which were pressed at 20 MPa, exhibits four diffraction arcs from the (200) plane in spite of the SAXS pattern showing the scattering maxima in the meridional direction (see the SAXS patterns a–d). The WAXD and SAXS patterns d together indicate that the *a*-axes are tilted at about 40° away from the surface normal of the mat face. The diffraction peak of the (020) plane in the horizontal direction was confirmed by a diffractometer. Judging from these diffraction arcs, the tilting is probably caused by slippage between crystals on the crystal b–c plane as a result of shear induced by the compressive stress during the sample preparation. This indicates that the *c*-axes are tilted at about 50° from the surface normal of the mat face. We also note in passing that the WAXD patterns of type I specimens were independent of the pressure used in preparing the films; the patterns were similar regardless of pressure up to 20 MPa.

Table I shows the characteristics of the mats prepared by the two methods described earlier in the Experimental Section. Both types of mats were pressed under a pressure of 20 MPa prior to the measurement. The crystallinity and melting point of the type II specimens are slightly higher than those of the type I specimens. However, the long period or the thickness of the crystal lamellae is somewhat shorter in the latter apparently because of tilting of the *c*-axes. As with the WAXD patterns, the results of type I specimens were not affected by the pressure that was applied during the film preparation (up to 20 MPa). The melting point was slightly higher in the type II specimens than in the type I specimens. It was also noted that the crystals were larger in the type II specimens than in the type I specimens.

Figure 3 shows the variation of WAXD and SAXS patterns (end view) for the type II specimens that had been pressed at 20 MPa. The specimens had been

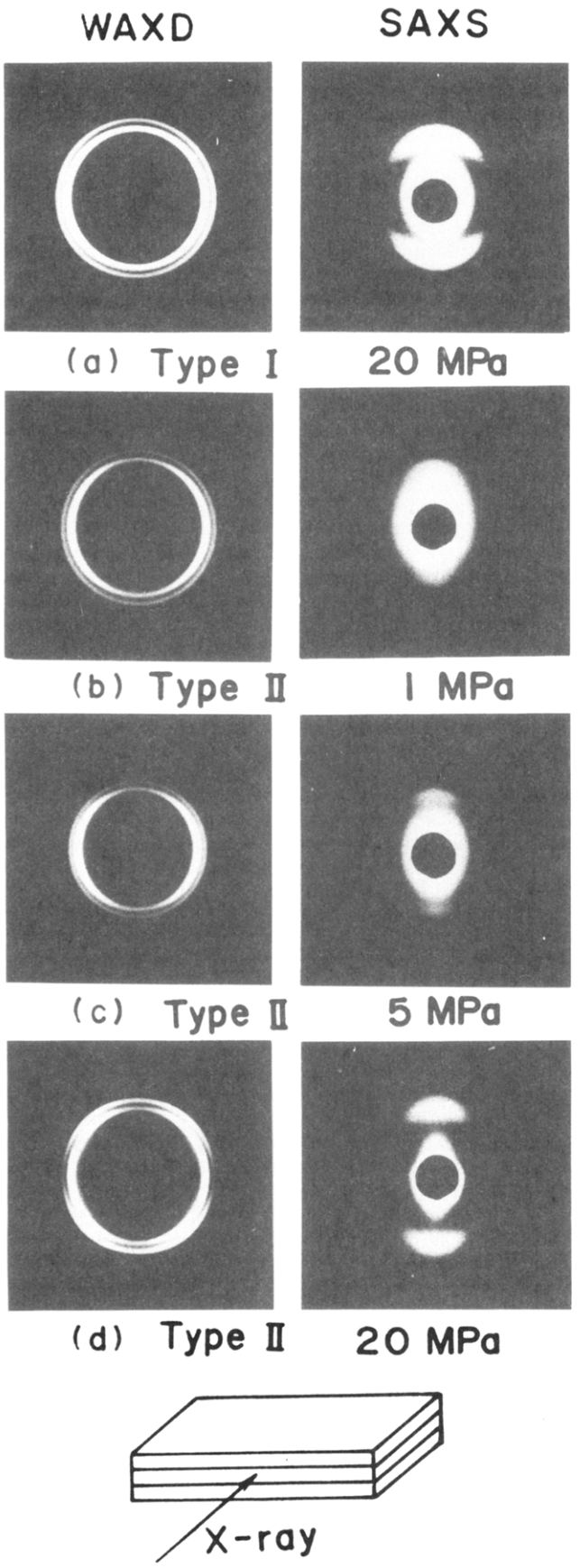


**Figure 2.** WAXD and SAXS patterns (end view) of types I and II single-crystal mats that were pressed at the indicated stresses.

annealed for 30 min at the indicated temperatures prior to the X-ray measurements. The WAXD pattern showed four diffraction arcs of the (200) planes when the temperature is below 120 °C, but the arcs become longer as the annealing temperature was increased. The SAXS pattern shows strong maxima in the meridional scattering. The scattering maxima are located close to the scattering center, and they become indistinguishable as the temperature was raised above 130 °C. It can be seen from the changes in the WAXD and SAXS patterns that the orientational disorder and thickness fluctuation of single-crystal mats become more pronounced as the fold period (long spacing) increases. The same trend was also observed in the type I mats and the type II mats that had been pressed at 1, 5, and 20 MPa.

**Table I. Crystallinity, Long Period, Lamella Thickness, and Melting Temperature of Types I and II Single-Crystal Mats (SGCM) That Had Been Pressed under 20 MPa at 20 °C**

| SGCM film | type I | type II |
|---|---|---|
| crystallinity (%) | 82.5 | 87.0 |
| long period (Å) | 140 | 123 |
| crystal lamella thickness (Å) | 116 | 107 |
| melting point (°C) | 134 | 136 |

Table II displays the effects of annealing on the crystallinity, the long period, and the maximum draw ratio of the types I and II mats. The annealing was performed over a period of 30 min at the temperatures indicated in the table. The type I specimens that were annealed at temperatures between 20 and 120 °C could be elongated only up to a draw ratio of 3–4 at 20 °C. This low draw ratio is to be compared with the corresponding value of 20 for the gel film that was annealed at 110 °C for 15 min before being stretched at room temperature.[17] The poor drawability indicates that the number of entanglement meshes to connect the mats by the annealing is not sufficient for the effective transfer of the drawing force between the molecules. It should also be noted that the deformation of the mats that had been annealed at temperatures below 130 °C was not uniform; at larger draw ratios, fine cracks developed on the film surface and the specimen, which was originally translucent, became white as a result of void formation. Observation under an optical microscope revealed that the drawn film consisted of two alternating zones, one being relatively undeformed and the other being highly drawn with cracks developing in several spots. For the films annealed at 140 °C, the deformation was almost similar to that of the melt films. This may be ascribed to a sharp drop in the crystallinity as a result of partial melting in the mats.

In contrast to the type I specimens, the type II specimens could not be elongated at 20 °C if the annealing temperature was below 130 °C. This is most likely due to the low level of entanglement within the type II specimens. On the other hand, the draw ratio of the specimen at 20 °C increased somewhat to 3–4 if the specimen was annealed at 140 °C, slightly above the melting point. This improved draw ratio may have resulted from an increase in the number of entanglement meshes brought about by partial melting. The latter would provide more and longer molecular segments in the amorphous phase, thereby increasing the chance of chain entanglement. Consequently, this result supports the hypothesis that the drawability strongly depends on the degree of entanglement as pointed out by Smith et al.[6] It was noted during the experiment that a draw ratio of 20 could be obtained in the type II specimen if the specimen was elongated at 120 °C after annealing at the same temperature. Despite this improvement, however, the drawability is still very poor when compared with the draw ratio of 150 for the type I specimens tested under the same conditions.

To further understand the effect of entanglement on the drawability, single-crystal mats were prepared ac-

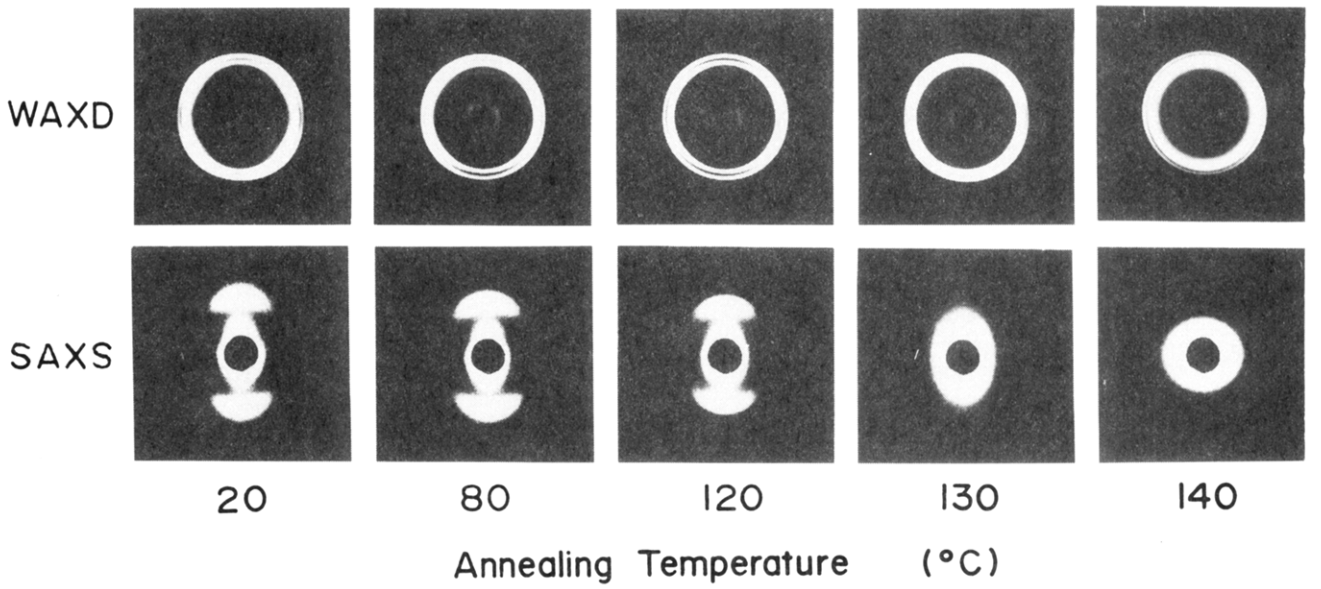


**Figure 3.** WAXD and SAXS patterns (end view) of type II single-crystal mats upon annealing at different temperatures.

**Table II. Effects of Annealing on Crystallinity, Long Period, and Maximum Draw Ratio for Types I and II Single-Crystal Mats**[a]

| | type I | | | | type II | | | |
|---|---|---|---|---|---|---|---|---|
| | | | max draw ratio, λ | | | | max draw ratio, λ | |
| annealing temp (°C) | crystallinity (%) | long period (Å) | cold-drawn (20 °C) | drawn at the annealing temp | crystallinity (%) | long period (Å) | cold-drawn (20 °C) | drawn at the annealing temp |
| 20 | 82.5 | 140 | (3–4) | | 87.0 | 123 | | |
| 80 | 84.0 | 140 | (3–4) | 80 | 89.0 | 125 | | |
| 120 | 83.5 | 140 | (3–4) | 150 | 89.5 | 132 | | 20 |
| 130 | 80.0 | 200 | (10) | 300 | 85.0 | 220 | | 70 |
| 140 | 57.0 | | 10 | 300 | 59.0 | | 3–4 | 150 |

[a] Type II mats had been pressed under 20 MPa at 20 °C. The symbol bracket denotes the highly drawn zone within the specimen.

cording to method I from a solution having a concentration of 0.01 g/100 mL. Their characteristics were compared with the corresponding data obtained from two types of specimens, i.e., (1) the mats prepared from a 0.1 g/100 mL solution and (2) the dried gel film prepared from an optimum 0.675 g/100 mL solution.

To obtain test specimens, the sheets of the type I mats and the gels were cut into strips of 22-mm length and 10-mm width. The strips were clamped in a manual stretching device in such a way that the length to be drawn was 4 mm. The specimens were placed in an oven at 135 °C and elongated manually to the desired draw ratio, λ (less than 100). Due to the limited size of the oven, elongation beyond λ = 100 was done in the first step and the drawn specimen was cut into strips of 70-mm length. These specimens, each clamped over a length of 10 mm at the end (the length to be stretched being 50 mm), were drawn to the desired ratio beyond λ = 100. After stretching, all specimens were quenched with a fixed dimension to room temperature.

Figure 4 shows the change in apparent crystallinity with the draw ratio λ for the three types of specimens. The experimental error was less than 1.0%. The gel film that was quenched at 0 °C and subsequently dried at 20 °C shows the highest draw ratio. For the specimens prepared from the 0.01 g/100 mL solution, the crystallinity decreases when the draw ratio is less than 20, apparently as a result of crystal transformation in which the folded chains convert to extended crystalline fibers. Significantly, this behavior is not observed in the other two types of specimens. While specimen prepared from the 0.01 g/100 mL solution has the highest crystallinity in the original (undrawn) state,

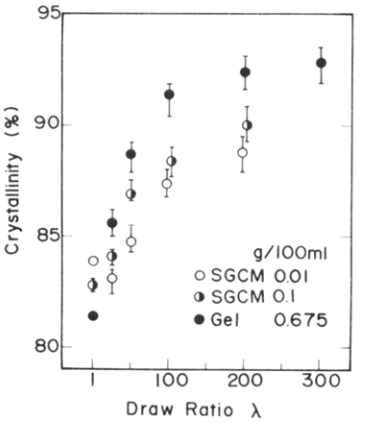


**Figure 4.** Crystallinity as a function of the draw ratio λ for type I single-crystal mats prepared from 0.01 and 0.1 g/100 mL solutions and gel films prepared from a 0.675 g/100 mL solution.

it has the lowest crystallinity at each draw ratio after drawing. These results imply that while the gel film had the optimum number of entanglement meshes for effectively transmitting the draw force between molecules, the specimen prepared from the 0.01 g/100 mL solution had the smallest number of entanglements and its drawability is somewhat attributed to slippage of molecular chains in the specimen.

In order to confirm the above result, these specimens were subjected to X-ray measurements for determination of their second-order orientation factor, $F_c$, of the *c*-axes. Figure 5 shows the results in which $F_c$ characterizes the distribution of crystalline orientation with a variation between $-1/2$ and +1. $F_c$ is 0 for random orientation, and

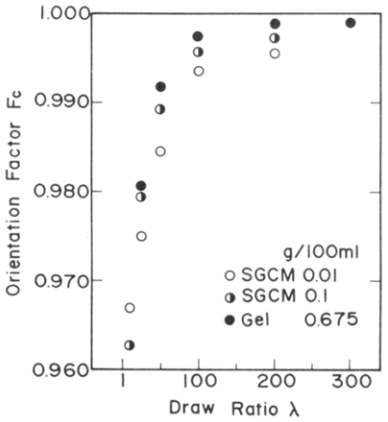


**Figure 5.** Orientation factor as a function of the draw ratio λ for type I single-crystal mats prepared from 0.01 and 0.1 g/100 mL solutions and gel films prepared from a 0.675 g/100 mL solution.

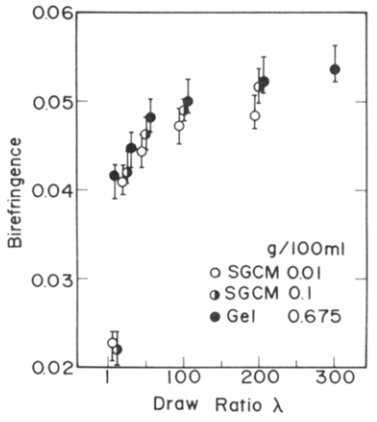


**Figure 6.** Birefringence as a function of the draw ratio λ for type I single-crystal mats prepared from 0.01 and 0.1 g/100 mL solutions and gel films prepared from a 0.675 g/100 mL solution.

it is unity if the *c*-axes are parallel to the stretching direction and $-1/2$ if they are perpendicular. The orientation factor was estimated from the orientation distribution factor of the (002) plane. The value increases with draw ratio λ and is close to unity beyond λ = 100, as has been reported previously.[3] Among the three specimens, the value of the dried gel film shows the most significant increase, while the mats prepared from the 0.01 g/100 mL solution consistently show the lowest value at each draw ratio. The latter may be attributed to the lack of a sufficient number of chain entanglements in the specimen; as a result, molecular orientation takes place by slippage of molecular chains in addition to sample deformation, thereby impeding the orientation of *c*-axes in the drawing direction during elongation. The above results corroborate well with the birefringence data which are shown in Figure 6. As can be seen from the figure, the gel film has the highest birefringence at each draw ratio while the mat film prepared from the 0.01 g/100 mL solution has the lowest.

Figure 7 shows the change of Young's modulus as a function of λ for the three types of specimens. The length of the specimen between the jaws was 40 mm and the width was about 2 mm. The specimens were elongated at 20 °C with an Instron type tensile tester at a cross-head speed of 10 mm·min$^{-1}$. The experimental uncertainty was shown by error bars in the figure. For λ greater than 100, the gel film had the greatest increase of Young's modulus; further, the film also had the highest values of the crystallinity, the second-order orientation factor, and the birefringence. These results indicate that the initial

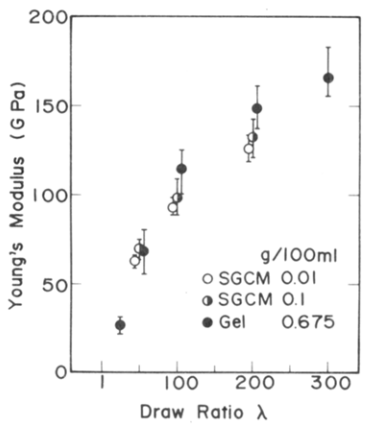


**Figure 7.** Young's modulus as a function of the draw ratio λ for type I single-crystal mats prepared from 0.01 and 0.1 g/100 mL solutions and gel films prepared from a 0.675 g/100 mL solution.

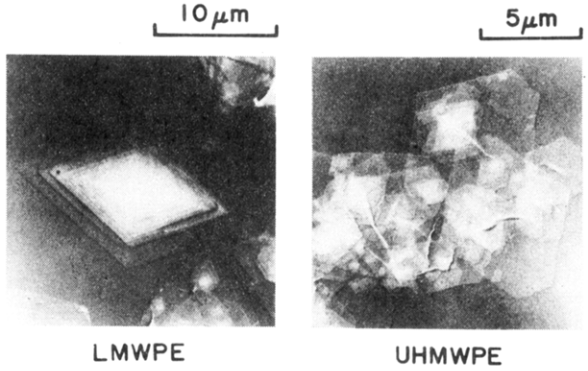


**Figure 8.** TEM photographs of LMWPE and UHMWPE single-crystal mats prepared from 0.01 g/100 mL solution according to method II.

entanglement density has a significant effect on the Young's modulus of drawn specimens, even if entanglement density is changed during elongation.

Figure 8 shows the TEM photographs for both the LMWPE and the UHMWPE single crystals which were prepared from the 0.01 g/100 mL solution by method II; these specimens had not been pressed prior to the TEM probe. The UHMWPE single crystals were irregular in shape as discussed by Schulz.[18] That is, they are truncated and have many more spiral growths per unit surface area, indicating a screw dislocation induced connectivity between crystal terraces. In contrast, the LMWPE single crystals appear rhombic as has been generally observed.[19] It should be noted that the UHMWPE could not be readily prepared in the single-crystal form; the UHMWPE specimen shown in Figure 8 had a molecular weight of $1 \times 10^6$; specimens with a high molecular weight, $3 \times 10^6$, could not be successfully prepared even in the form shown in Figure 8. Thus, while the LMWPE single crystals clearly show the existence of the regular-folded chain loops, the UHMWPE specimens do not provide any such information. Nevertheless, the irregular-shaped mats of the UHMWPE specimens may very well be associated with the formation of entanglement meshes between the mats. In fact, as noted earlier, while the LMWPE mats prepared by method I could not form films, the UHMWPE mats could be made into films with a morphology similar to that of the dried gel film, as shown in Figure 1. Consequently, it is quite possible that when single crystals of UHMWPE were formed in the solution, the mats were connected with each other by mutual entanglement of molecules. This is probably why the mat film appeared spongy upon evaporation of the solvent and subsequently

it could be drawn up to 300 times. Apart from the concept of entanglement meshes, the screw dislocation induced connectively between crystal terraces observed in Figure 8 provides such an another possibility that the greater connectedness promotes the greater drawability of UHMWPE single-crystal mats.

Returning to Table II, it should be noted that, in spite of the annealing at 130 °C, the type II mats had no drawability at 20 °C. The introduction of ethanol and the subsequent stirring of the solution probably prevented the formation of chain links between the mats. Here, we must emphasize that compressed specimens of UHMWPE single-crystal mats with the screw dislocation could not be elongated at room temperature without the annealing at 140 °C, slightly above the melting point. This implies the importance of mutual entanglement of molecules to connect the mats to each other. It is therefore quite conceivable that a sufficient number of entanglements remained within the gel film after it underwent the quenching and drying processes. These results indicate the hypothesis that chain entanglements play one of the most important roles in the high drawability of these films, as suggested by Smith et al.[6]

## Conclusion

The single-crystal mats (the type I specimens) of UHMWPE prepared by method I were found to behave in a manner similar to the dried gel film rather than to the single-crystal mats of LMWPE. Its maximum draw ratio reached 200; by contrast, the drawability of single crystals (the type II specimens) prepared by method II was much poorer. The cause for this difference has been attributed to the number of entanglement meshes, which was much less in the type II specimens than in the type I specimens. Even for the type I specimens, the Young's modulus and the molecular orientation were lower when the mats were prepared from solutions having a concentration much less than the optimum value of 0.675 g/100 mL. This indicates that the number of entanglements within the type I specimens prepared from solution with a concentration of 0.01 g/100 mL was much fewer than the most suitable number of entanglements within the gels prepared from the solution with the critical concentration and, consequently, their molecular chains within the type I specimens were somewhat obliged to slip relative to each other instead of orienting themselves during elongation. It may be concluded, therefore, that the number of entanglements plays one of the critical roles in the drawability, in agreement with the concept proposed earlier by Smith et al.

**Acknowledgment.** We are grateful to Prof. T. T. Wang of Rutgers University for kindly reading the manuscript and making numerous suggestions. We are also indebted to Mr. Akira Kubotsu of Central Research Laboratories, Kuraray Co., Ltd., for taking the TEM photographs of our single-crystal mats of LMWPE and UHMWPE.

## References and Notes

(1) Smith, P.; Lemstra, P. J. *J. Mater. Sci.* **1980**, *15*, 505.
(2) Smith, P.; Lemstra, P. J.; Pijpers, J. P. L.; Kiel, A. M. *Colloid Polym. Sci.* **1981**, *259*, 1070.
(3) Matsuo, M.; Sawatari, C. *Macromolecules* **1986**, *19*, 2036.
(4) Furuhata, K.; Yokokawa, T.; Miyasaka, K. *J. Polym. Sci., Polym. Phys. Ed.* **1984**, *22*, 133.
(5) Kanamoto, T.; Tsuruta, A.; Tanaka, K.; Porter, R. S. *Polym. J.* **1983**, *15*, 327.
(6) Smith, P.; Lemstra, P. J.; Booij, H. C. *J. Polym. Sci., Polym. Phys. Ed.* **1981**, *19*, 877.
(7) Ogita, T.; Yamamoto, R.; Suzuki, N.; Ozaki, F.; Matsuo, M. *Polymer* **1991**, *32*, 822.
(8) Statton, W. O. *J. Appl. Phys.* **1967**, *38*, 4149.
(9) Ishikawa, K.; Miyasaka, K.; Maeda, M. *J. Polym. Sci., Polym. Phys. Ed.* **1969**, *7*, 2029.
(10) Maeda, M.; Miyasaka, K.; Ishikawa, K. *J. Polym. Sci., Polym. Phys. Ed.* **1970**, *8*, 355.
(11) Maeda, M.; Miyasaka, K.; Ishikawa, K. *J. Polym. Sci., Polym. Phys. Ed.* **1970**, *8*, 1865.
(12) Sawatari, C.; Okumura, T.; Matsuo, M. *Polym. J.* **1986**, *18*, 741.
(13) Ogita, T.; Suzuki, N.; Kawahara, Y.; Matsuo, M. *Polymer* **1992**, *33*, 698.
(14) Ogita, T.; Suzuki, N.; Ozaki, F.; Sawatari, C.; Matsuo, M. *Sen-i Gakkaishi* **1990**, *46*, 481.
(15) Bunn, C. W. *Trans. Faraday Soc.* **1939**, *35*, 482.
(16) Sawatari, C.; Shimogiri, S.; Matsuo, M. *Macromolecules* **1987**, *20*, 1033.
(17) Matsuo, M.; Manley, R. St. J. *Macromolecules* **1983**, *16*, 1500.
(18) Schultz, J. *Polymer Materials Science*; Prentice-Hall: Englewood Cliffs, NJ, 1974; pp 37 and 38.
(19) Keller, A. *Growth and Perfection of Crystals*; Turnbell, D., Ed.: John Wiley & Sons: New York, 1958.